Stability and Unfolding of Reduced *Escherichia coli* Glutaredoxin 2: A Monomeric Structural Homologue of the Glutathione Transferase Family[†]

Samantha Gildenhuys, Louise A. Wallace,[‡] and Heini W. Dirr*

Protein Structure-Function Research Unit, School of Molecular and Cell Biology, University of the Witwatersrand, Johannesburg 2050, South Africa

Received July 7, 2008; Revised Manuscript Received August 12, 2008

ABSTRACT: Glutaredoxin 2 (Grx2) from *Escherichia coli* is monomeric and an atypical glutaredoxin that takes part in the monothiol deglutathionylation of proteins. Unlike its orthologs, Grx2 is a larger molecule with a canonical glutathione transferase (GST) fold that consists of two structurally distinct domains, an N-terminal glutaredoxin domain and a C-terminal α-helical domain. While GSTs are dimeric proteins, the conformational stability and unfolding kinetics of Grx2 were investigated to establish the contribution made by the domain interface to the stability of the tertiary structure of GST-like proteins without any influence from quaternary interactions. Equilibrium unfolding transitions for Grx2, using urea as a denaturant, are monophasic and exhibit coincidence of the fluorescence and CD data indicative of a concerted loss or formation of tertiary and secondary structure. The data fit well to a two-state N ↔ U model with no evidence that an intermediate is being formed. The experimental *m* value [2.7 kcal mol^{-1} (M urea)$^{-1}$] is in excellent agreement with a predicted value of 2.5 kcal mol^{-1} (M urea)$^{-1}$ based on the amount of surface area expected to become exposed during unfolding. These findings provide evidence that the two structurally distinct domains of Grx2 behave as a single cooperative folding unit. The unfolding kinetics are complex which, as a result of native-state heterogeneity, are characterized by two observable unfolding reactions that occur in parallel. A major population representing one distinct nativelike form unfolds on a fast track to denatured Grx2 with *cis*-Pro49. This is followed by a spectroscopically silent *cis*−*trans* proline isomerization reaction as determined by interrupted unfolding experiments. A minor population representing the other distinct nativelike form unfolds slowly with its rate being limited by an undetermined structural isomerization reaction. Further, there is no evidence indicating that unfolding proceeds via a high-energy intermediate that might suggest independent unfolding of the two nonidentical domains in Grx2. The kinetics data are, therefore, consistent with the existence of cooperativity between the domains, in agreement with the equilibrium data.

The glutathione transferase (GST)[1] fold represents a large family of monomeric and dimeric intracellular proteins (http://scop.mrc-lmb.cam.ac.uk/scop/data/scop.b.b.fh.b.A.html) that perform a wide range of catalytic and noncatalytic functions (for reviews, see refs *1* and *2*). The canonical GST fold possesses two structural domains: a thioredoxin/glutaredoxin-like N-terminal domain (domain 1) and a larger, unique all-α-helical C-terminal domain (domain 2) (*3*), as illustrated in Figure 1. The active sites of these multidomain proteins are located along the interface between the two domains with each domain contributing to overall protein function. The dynamic behavior of the domain interface also determines functional selectivity (*4*). Domain 1 is thought to have been recruited from a thioredoxin-like ancestral protein (*3, 5*), which, following the addition of all-α-helical domain 2, gave rise to a monomeric intermediate in the evolutionary pathway of the canonical dimeric GSTs (*6, 7*). Conformational stability data for dimeric GSTs together with their proposed evolutionary pathways suggest that the subunits of the "older" GSTs are more stable than those of the "newer" GSTs (*8*). As the dimer interface evolved, intersubunit interactions contribute increasingly to the stability of the individual subunits (*8, 9*). Although the structures and functions of the GST family have been studied extensively, little is known about the contribution made by the domain interface to the stability and folding of individual GST subunits. GSTs being two-domain, dimeric proteins have four components that contribute to their overall stability: the intrinsic stabilities of the two nonidentical domains, the interactions at the domain−domain interface, and the interactions across the dimer interface. Complicating the determination of how domain interactions contribute to the stability of GST subunits is the presence of quaternary interactions

[†] This work was supported by the University of the Witwatersrand, South African National Research Foundation Grant 205359, the South African Research Chairs Initiative of the Department of Science and Technology, and National Research Foundation Grant 64788.

* To whom correspondence should be addressed. Phone: +27117176352. Fax: +27117176351. E-mail: heinrich.dirr@wits.ac.za.

[‡] Current address: Genencor, A Danisco Division, 925 Page Mill Rd., Palo Alto, CA 94304.

[1] Abbreviations: CD, circular dichroism; DCIP, 2,6-dichloroindophenol; DTT, dithiothreitol; Grx2, glutaredoxin 2; hFKBP, human FK506-binding protein; GST, glutathione transferase; k_u, rate constant for unfolding; PPI, peptidyl-prolyl isomerase; ΔSASA, change in solvent accessible surface area; SCOP, Structural Classification of Proteins; SE-HPLC, size exclusion high-performance liquid chromatography; UV, ultraviolet; Xaa, any amino acid.

10.1021/bi801272t CCC: $40.75
Published on Web 09/13/2008

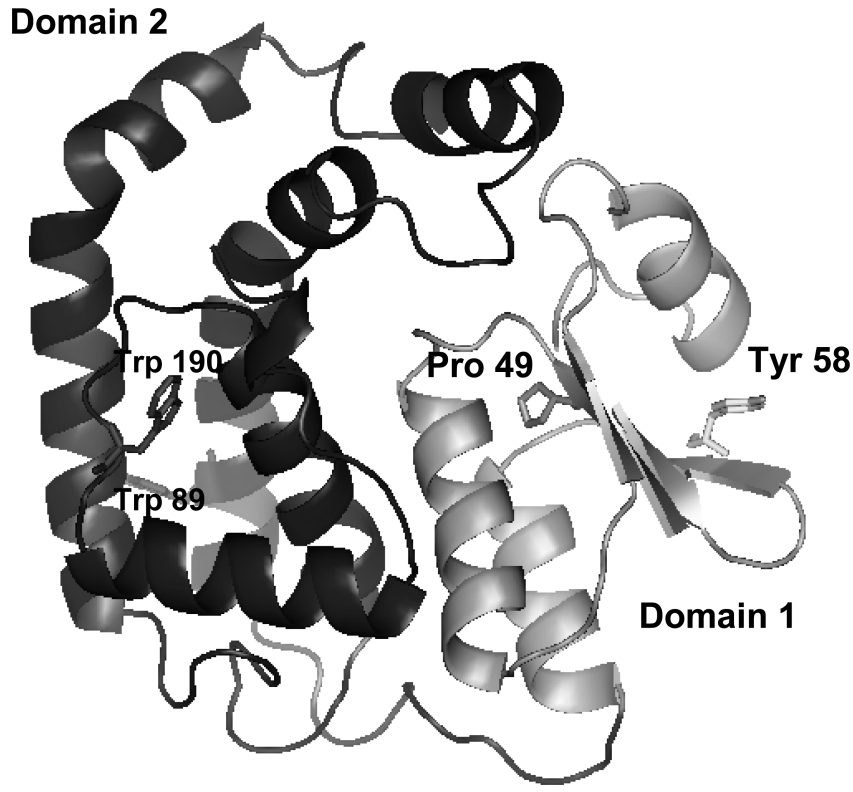

FIGURE 1: Structure of Grx2 (PDB entry 1G7O) showing the two domains, *cis*-proline 49, tryptophan 89, tryptophan 190, and tyrosine 58. The image was created using PyMOL (*31*).

which include residues involved in interdomain contacts (*10*). Further, the conventional default hypothesis is that protein domains are autonomous folding−unfolding units (*11*). Recently, hydrogen exchange mass spectrometry has revealed that domain 1 is conformationally more flexible than domain 2 in class mu GST (*12*).

To improve our understanding of the stability, folding, and assembly of GST monomers in the absence of quaternary interactions, we have studied the stability and unfolding of glutaredoxin 2 (Grx2) from *Escherichia coli*, a monomeric GST-like protein (*6*). Tryptophan fluorescence and far-UV circular dichroism were employed to monitor urea-induced structural changes at equilibrium, while unfolding kinetics were determined by fluorescence stopped-flow single- and double-jump experiments. The components that should contribute to its stability are the intrinsic stabilities of the two nonidentical domains and the interactions at the domain interface. Grx2 is an atypical glutaredoxin that participates mainly in monothiol reactions that remove glutathionylation from proteins (*6, 13*). Structurally, Grx2 (see Figure 1) displays the greatest similarity to the theta and omega class GSTs, which are suggested to represent ancestral dimeric precursors of other canonical GSTs (*7, 14*). Like all GST-like proteins, Grx2 has a conserved *cis*-proline residue in domain 1 (Figure 1). Grx2 is functionally related to the omega GSTs in that both participate in redox chemistry (*6, 7*). A monomeric Grx2-like protein may represent an intermediate in the evolutionary pathway of the canonical GSTs (*6, 7*).

MATERIALS AND METHODS

Materials. Ultrapure (99.5%) urea was purchased from BDH laboratory supplies (Poole Dorset, U.K.). DEAE-Sepharose and DCIP were purchased from Sigma (St. Louis, MO). All other reagents were analytical-grade. Purified hFKBP-12 was a generous gift from J.-U. Rahfeld (EMBL, Heidelberg, Germany).

Plasmids and Mutagenesis. The pET24a plasmid encoding the cDNA sequence for Grx2 was a generous gift from J. Dyson (The Scripps Institute, La Jolla, CA) (*6*). The Y58W mutant was generated using the QuikChange site-directed mutagenesis kit from Stratagene (La Jolla, CA), where the Y codon (TAT) was altered to the W codon (TGG). Sequencing by Inqaba Biotechnical Industries (Pty) Ltd. (Pretoria, South Africa) confirmed the incorporation of the TGG codon without other mutations.

Protein Expression and Purification. Wild-type Grx2 was overexpressed in BL21(DE3)pLysS cells containing the pET24a plasmid (*6, 13*). Y58W Grx2 was expressed in BL21(DE3) cells containing the pET24a plasmid encoding the mutant protein. Both proteins were expressed and purified using DEAE-Sepharose anion exchange chromatography as previously described (*6, 13*). The purity of the proteins was assessed using SDS−PAGE and SE-HPLC. Purified Grx2 forms were dialyzed and then either snap-frozen at −70 °C or used within 1 week of dialysis. The dialysis buffer was 50 mM sodium phosphate (pH 7) containing 50 mM sodium chloride, 1 mM DTT, and 0.02% sodium azide. Unless otherwise stated, the dialysis buffer was used for all experiments. The concentration of wild-type Grx2 or Y58W-Grx2 was determined spectrophotometrically, using an extinction coefficient of 21680 M^{-1} cm^{-1} (*13*) or 27670 M^{-1} cm^{-1} at 280 nm, respectively. The extinction coefficient for Y58W-Grx2 was calculated using the method described by Perkins (*15*).

Equilibrium Studies. Unfolding of Grx2 (5 μM) in 50 mM sodium phosphate (pH 7) containing 50 mM sodium chloride,

1 mM DTT, and 0.02% sodium azide was conducted at 20 °C over a range of urea concentrations (0−8 M). Structural changes were monitored by far-UV CD and tryptophan fluorescence (excitation at 295 nm). Buffer contributions were subtracted from all data. Rayleigh scattering was used to monitor aggregation (excitation and emission at 295 nm).

Kinetics Measurements. Unfolding kinetics experiments were conducted in an Applied Photophysics (Leatherhead, U.K.) BioSequential SX-18MV stopped-flow fluorimeter (dead time of 2 ms) with a Peltier temperature control unit. Excitation was at 280 nm, and the emission intensity was monitored using a 320 nm cutoff filter. The buffer was 50 mM sodium phosphate (pH 7) containing 50 mM sodium chloride, 1 mM DTT, and 0.02% sodium azide.

Data Analysis. Equilibrium unfolding data were fitted to a two-state model (N ⇆ U) (*16*). The free energy of unfolding in the absence of denaturant, $\Delta G(H_2O)$, and the susceptibility of the protein to denaturant (the *m* value) were calculated using the linear extrapolation method (*16*). Kinetic traces were analyzed and fitted by a nonlinear least-squares method using the Applied Photophysics software version 4.47. Residual plots were used to assess the accuracy and quality of the fits.

RESULTS

Probes for Monitoring Structural Changes during Unfolding. The Grx2 structure consists of two nonidentical domains (Figure 1). Domain 1 (residues 1−71) has no tryptophan residues and contains 21% of the total secondary structure (29 residues in α-helices and 17 residues in β-strands). Domain 2 (residues 84−215) has two tryptophans (Trp89 and Trp190) and contains 79% of the total secondary structure (85 residues in α-helices and three residues in β-strands). Grx2 displays a far-UV CD spectrum with ellipticity minima at 208 and 222 nm that is typical of a predominantly helical protein (Figure 2A). Since most of the protein's secondary structure is found in domain 2, the signal measured at 222 nm will report primarily on structural changes in this domain. Fluorescence measurements of wild-type Grx2 will follow the tertiary structure around the two tryptophan residues in domain 2. A maximum emission wavelength of 340 nm (Figure 2B) is consistent with the partial burial of both tryptophans in the structure of folded Grx2. Should the two domains unfold independently of one another, the unfolding of domain 1 will be invisible to fluorescence measurements. Therefore, the Y58W mutant of Grx2 was generated to introduce a tryptophan into domain 1 so that tertiary structural changes in this domain can be followed by fluorescence. The location of Tyr58 is shown in Figure 1. The nondisruptive nature of the Y58W mutation is demonstrated by far-UV CD data (Figure 2A). Trp58 contributes approximately one-fifth of the total fluorescence of the native mutant, which also displays a maximum emission wavelength of 340 nm. Unfolding of Grx2 is accompanied by a decrease in fluorescence intensity and a red shift in the maximum emission wavelength to 355 nm (Figure 2B).

Equilibrium Unfolding of Grx2. Urea-induced unfolding of Grx2 was monitored with far-UV CD (secondary structure probe) and tryptophan fluorescence (tertiary structure probe). The unfolding transitions for wild-type Grx2 are sigmoidal

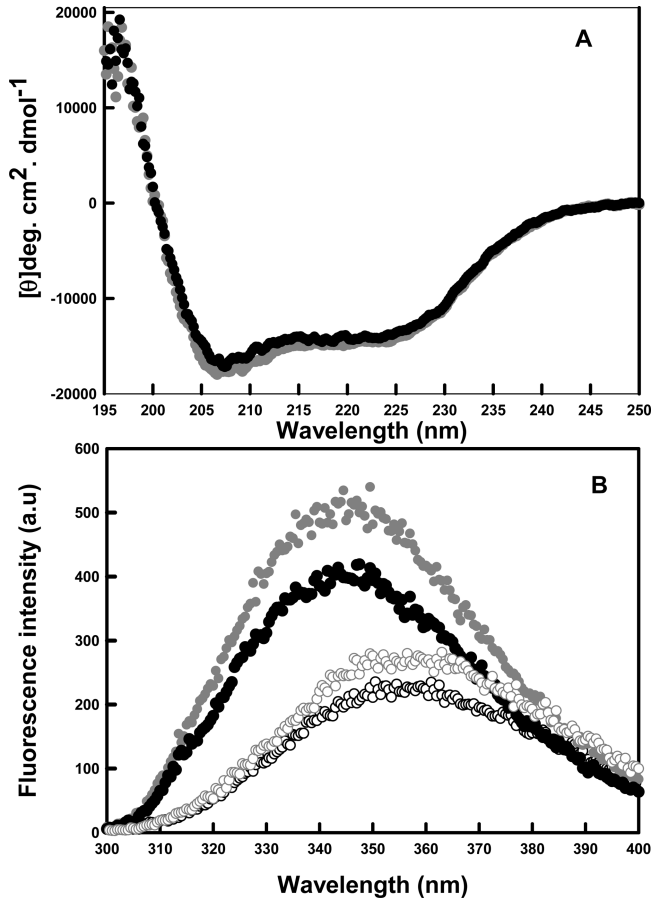

FIGURE 2: Far-UV CD spectra (A) and tryptophan fluorescence emission spectra (B) with excitation at 295 nm and for 5 μM wild-type (●) and Y58W Grx2 (gray circles). Fluorescence emission spectra were also obtained for denatured (7 M urea) wild-type Grx2 (○) and Y58W Grx2 (dotted circles).

and monophasic and display coincidence of the fluorescence and CD data (Figure 3A,B). The absence of unfolding and refolding hysteresis was demonstrated by refolding urea-denatured Grx2 to intermediate concentrations of urea. This yielded refolding transitions that superimposed with the unfolding curves (Figure S1 of the Supporting Information). The recoveries of fluorescence and CD signals were greater than 95 and 97%, respectively (Figure S2 of the Supporting Information). Further, the unfolding transitions were insensitive to protein concentration (1−100 μM), as expected for the unfolding of a monomeric protein without the involvement of higher-order states (not shown).

Coincidence of unfolding transitions for wild-type Grx2 obtained from fluorescence and CD data is evidence of a concerted loss or formation of tertiary and secondary structure. As the spectroscopic signals originate only (fluorescence) or primarily (CD) from domain 2 (see above), it is possible that should the two domains behave independently, the transitions are reporting only on structural changes in domain 2. However, the unfolding transitions of Y58W Grx2 that has a tryptophan residue engineered into domain 1 are also monophasic and display coincidence of fluorescence and CD data (Figure 3C,D). There is no indication that an intermediate is being formed as this would give rise to nonsuperimposable transitions for the two spectroscopic probes. These findings together with the data fitting parameters (e.g., *m* value) and the kinetic data described below

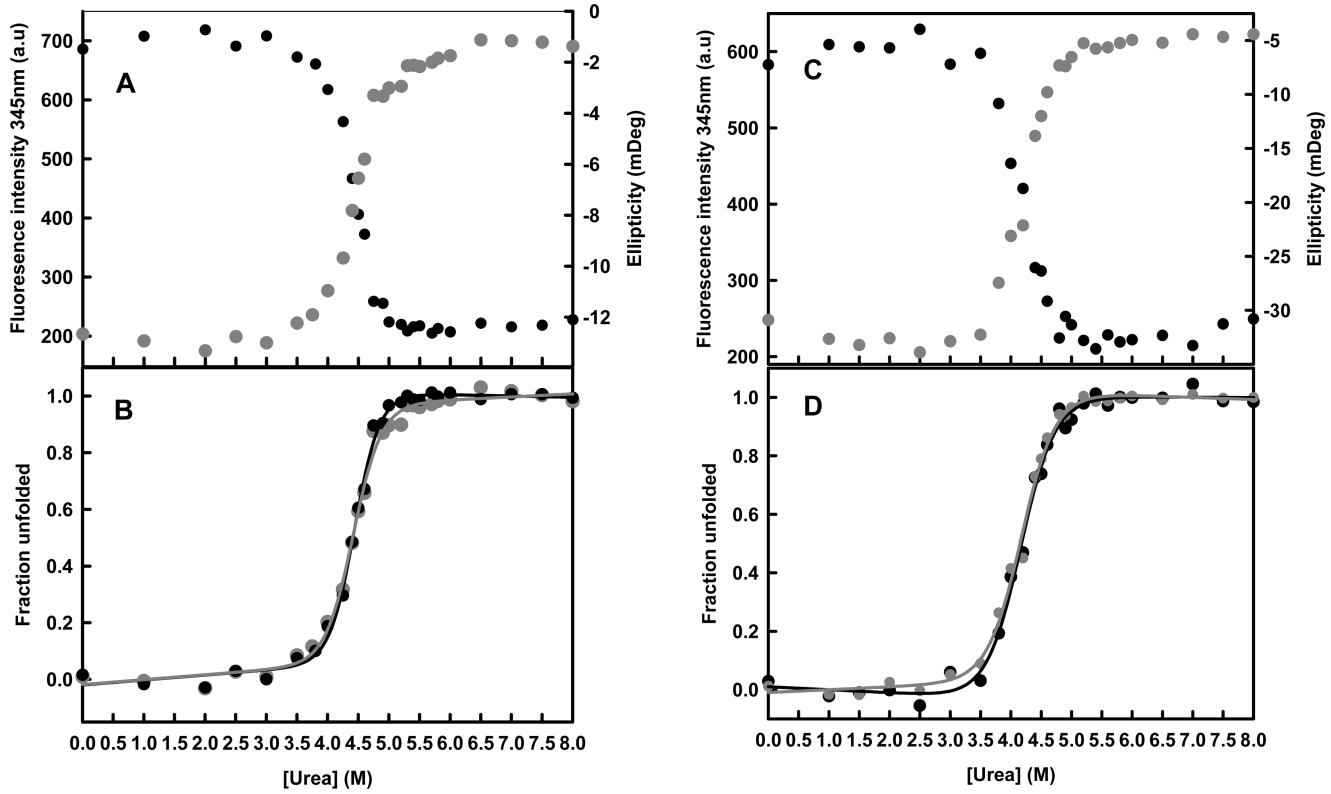

FIGURE 3: Urea-induced equilibrium unfolding of 5 μM wild-type Grx2 (A and B) and 5 μM Y58W Grx2 (C and D) as monitored by far-ultraviolet circular dichroism (gray circles) ellipticity at 222 nm and tryptophan fluorescence (●) (excitation wavelength of 295 nm and emission monitored at 345 nm). The solid lines represent fits to a two-state model. All measurements were taken at 20 °C, and the buffer was 50 mM phosphate (pH 7.0) containing 50 mM NaCl and 2 mM DTT.

provide evidence of cooperativity between the two domains and evidence that Grx2 behaves as a single cooperative unit.

Data fitting indicates that the unfolding of wild-type Grx2 is described well by a two-state (N ↔ U) model (solid line, Figure 3B) and not a three-state (N ↔ I ↔ U) model. The fit yields a C_m of 4.4 ± 0.1 M urea, a $\Delta G(H_2O)$ of 12.0 ± 1.0 kcal/mol, and an m value of 2.7 ± 0.2 kcal mol^{-1} (M urea)$^{-1}$. The experimental m value is in agreement with a predicted value of 2.5 kcal mol^{-1} (M urea)$^{-1}$ based on the size of Grx2 (215 residues) and the change in its solvent accessible surface area (ΔSASA = 19100 Å^2) upon unfolding (*17*). Should the two domains unfold as separate noncooperative units, the unfolding transition for each domain would have an m value determined by its ΔSASA of unfolding. For domains 1 and 2, the predicted m values are 1 kcal mol^{-1} (M urea)$^{-1}$ (ΔSASA = 5700 Å^2) and 1.6 kcal mol^{-1} (M urea)$^{-1}$ (ΔSASA = 11400 Å^2), respectively, which are significantly lower than that determined experimentally. Therefore, the agreement between the experimental and predicted m values is indicative of cooperative folding of Grx2 without the presence of intermediates (*18*). The unfolding data for the Y58W mutant were also described well by a two-state model yielding a C_m of 4.2 ± 0.1 M urea, a $\Delta G(H_2O)$ of 8.7 ± 0.8 kcal/mol, and an m value of 2.1 ± 0.2 kcal mol^{-1} (M urea)$^{-1}$, indicating that the substitution was slightly destabilizing.

Single-Jump Unfolding Kinetics. The unfolding of Grx2 under strong denaturing conditions (5−7.5 M urea), monitored by tryptophan fluorescence, follows biexponential kinetics irrespective of whether tryptophan residues are present only in domain 2 (wild-type) or in both domains (Y58W mutant) (panel A or B of Figure 4, respectively). The initial and final amplitudes are as predicted by equilibrium experiments, indicating that no burst phase occurs within the dead time. The time constants for the fast and slow unfolding phases for wild-type Grx2 in 6 M urea are 11.7 and 108 s, respectively, with 81% of the amplitude change occurring during the fast phase. The fast and slow phases of the Y58W mutant in 6 M urea display unfolding time constants of 1.73 and 147 s, respectively, with 92% of the total amplitude occurring during the fast phase. The logarithm of the rate constant of the major, fast phase increases linearly with urea concentration, while that of the minor, slow phase appears to be independent of urea (Figure 5). The fast unfolding data fit well to the linear equation $\log k_u = \log k_u(H_2O) + (m_u^{\ddagger}/2.303RT)[\text{urea}]$, where k_u is the rate constant for unfolding at a urea concentration ([urea]) and $k_u(H_2O)$ is the rate constant of unfolding in water. $m_u^{\ddagger}$ is the m value for the activation process from N to the transition state. The fits to the fast unfolding data in Figure 5 yield $k_{u,f}(H_2O)$ and $m_{u,f}^{\ddagger}$ values of 0.009 ms^{-1} and 0.89 kcal mol^{-1} (M urea)$^{-1}$ for wild-type Grx2 and 0.044 ms^{-1} and 0.91 kcal mol^{-1} (M urea)$^{-1}$ for its Y58W mutant, respectively. The corresponding fractional changes in solvent exposure between the native state and the rate-determining transition state for unfolding are 0.33 and 0.44 for the wild-type and Y58W mutant, respectively. These values were calculated from the ratio $m_u^{\ddagger}/m_{equil}$, where m_{equil} is the m value obtained from equilibrium studies.

As both tryptophan residues in wild-type Grx2 are located in domain 2, unfolding followed by fluorescence could reflect changes in only this domain. However, two phases are also observed for the Y58W mutant; the additional tryptophan did not result in new "domain 1-only" unfolding phases. The

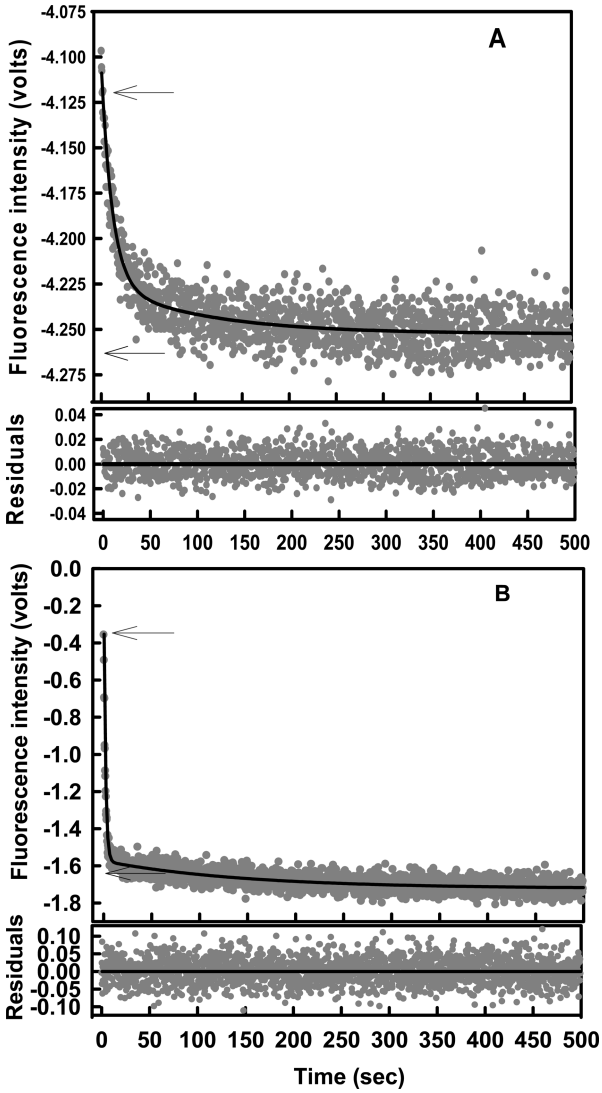

FIGURE 4: Kinetic unfolding traces for (A) wild-type Grx2 and (B) Y58W Grx2 monitored by tryptophan fluorescence at 20 °C. Both proteins were at a final concentration of 5 μM in 6 M urea. Solid lines represent fits to a biexponential equation, the bottom panel showing residuals for the fit. The arrows represent the positions of the native and unfolded baselines.

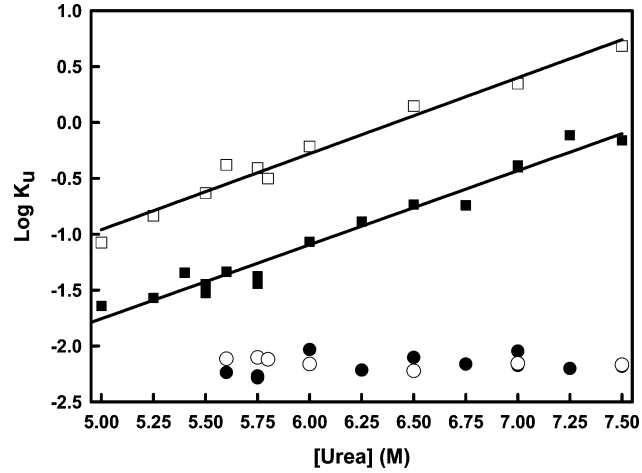

FIGURE 5: Urea dependence of the unfolding of wild-type Grx2 (black symbols) and Y58W Grx2 (white symbols). The dependencies of the (■ and □) fast phase and the (○ and ●) slow phase of unfolding were obtained from double-exponential fitting of the traces obtained at each urea concentration. The solid lines represent linear fits to the fast phase rate data with R^2 values of 0.96 and 0.97 obtained for wild-type and Y58W Grx2, respectively.

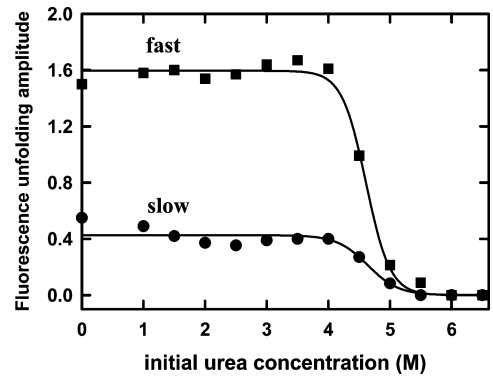

FIGURE 6: Unfolding initial conditions test conducted using different initial urea concentrations (0−6.5 M urea) while the final urea concentration was held at 6.5 M. The dependencies of the amplitudes on the initial urea concentration for the fast (■) and slow (●) phases were then plotted.

increased amplitude of the major fast phase suggests that it can be attributed to the unfolding of both domains. Further, when compared with that of wild-type Grx2, the increased rate of the faster unfolding phase of the Y58W mutant is most likely due to the destabilization of domain 1 expected upon the mutation of a tyrosine with a bulkier tryptophan residue. The kinetics data are consistent with the highly cooperative behavior between the domains observed in the equilibrium studies.

Since two unfolding phases are observed for Grx2, the possibility of them occurring either sequentially or in parallel was investigated by performing initial conditions tests (*19*). Different initial urea concentrations were used (0−6.5 M urea) while the final urea concentration was held at 6.5 M. The dependence of the rate constants and amplitudes of the unfolding reaction on the initial urea concentrations was determined by relying on the fact that rate constants depend only on the final conditions while amplitudes depend on both the initial and final conditions (*19, 20*). The amplitude data shown in Figure 6 indicate that unfolding remains biphasic at all initial urea concentrations while the rate constants were independent of the initial concentration of urea (not shown). Because the relative amplitudes of the unfolding phases represent the fraction of molecules present at the beginning of the reaction (*21*), the simultaneous presence of two unfolding phases with midpoints near that of the equilibrium unfolding transition indicates that the two unfolding reactions occur independently and, thus, run in parallel.

Interrupted Unfolding Kinetics (N → U → N). When Grx2 is unfolded to equilibrium at 6 M urea, single-jump experiments show that its refolding at 1 M urea is triphasic, with time constants of 61 ms, 0.79 s, and 180 s for the fast, medium, and slow reactions, respectively (Figure 7). In the interrupted unfolding experiments, Grx2 was unfolded in 6 M urea for different delay times before it was allowed to refold at 1 M urea. At short unfolding delay times (<10 s), refolding is biphasic with the fast and medium phases accounting for ~80 and ~20% of the total amplitude, respectively (Figure 8). This confirms the presence of two native-state species of Grx2, as discussed above. For longer delay times, a slow refolding phase develops with its amplitude increasing exponentially to 30% (time constant of 86 s). In a reciprocal manner, the amplitude of the fast

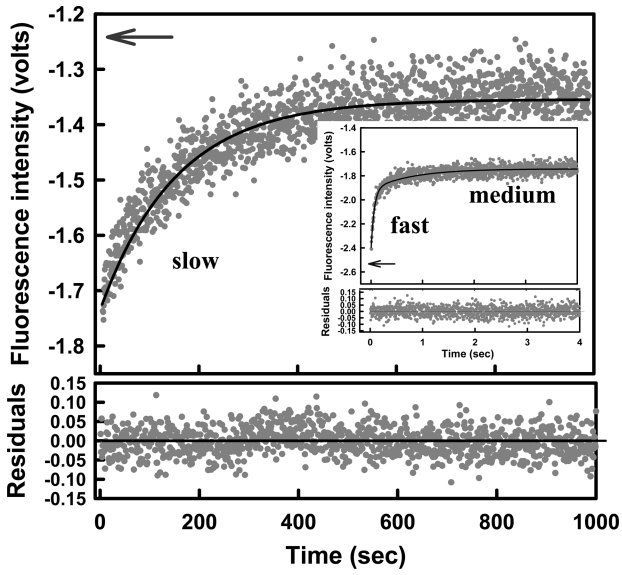

FIGURE 7: Refolding trace for wild-type Grx2 monitored by tryptophan fluorescence at 20 °C. Grx2 was unfolded in 6 M urea and then refolded in 1 M urea. The final protein concentration was 5 μM. Solid lines represent biexponential (inset; fast and medium phases) and single-exponential (slow phase) fits. Bottom panels show the residuals of the fits. The arrows represent the positions of the native and unfolded baselines.

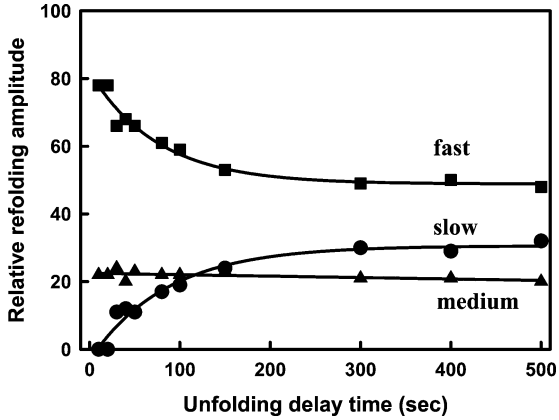

FIGURE 8: Double-jump refolding. Refolding amplitudes of 5 μM wild-type Grx2 at 1 M urea after unfolding delay periods in 6 M urea. Amplitudes for the (■) fast, (▲) medium, and (●) slow phases of refolding were obtained from the kinetic refolding data following each unfolding delay time. Solid lines represent single-exponential (fast and slow phase) and linear (medium phase) fits to the data.

phase decreases exponentially to 50% (time constant of 75 s). The amplitude of the medium phase is, however, not affected by the time of unfolding, and its relative amplitude remains constant at ~20%. The reciprocal variation of the amplitudes for the fast and slow phases, together with their time constants, is consistent with *cis*−*trans* proline isomerization occurring in the denatured state during the longer unfolding times (*22*). Native Grx2 has 12 X−Pro peptide bonds, one of which, Val48−Pro49, is in the *cis* configuration (*6*). The interrupted unfolding experiment suggests that unfolded Grx2 molecules with a *cis*-Pro49 fold along the fast direct track while Grx2 molecules with a *trans*-Pro49 follow a slow proline-limited folding track. The slow refolding reaction is significantly accelerated by the presence of the peptidyl prolyl isomerase hFKBP-12 (Figure 9), confirming that it is limited by the rate of proline isomerization, most likely involving Pro49. In the subsequent 500 s, most of the unfolded Grx2

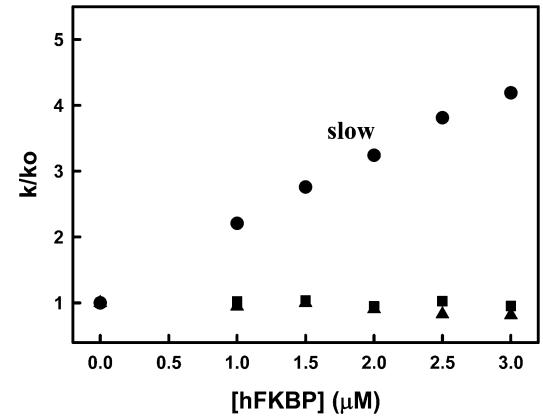

FIGURE 9: Effect of hFKBP-12 (a peptidyl prolyl isomerase) on the rates of the fast (■), medium (▲), and slow (●) phases. The k/k_o ratio was calculated by taking the rate of the refolding phase in the presence (k) of PPI divided by the rate of the same phase in the absence (k_o) of PPI. Final refolding conditions were 5 μM Grx2 in 1 M urea with 0−3 μM hFKBP-12.

molecules experience *cis*−*trans* isomerization, reaching an equilibrium mixture in which ~50% of the unfolded molecules possess *cis*-Pro49 and 30% possess *trans*-Pro49 (Figure 8).

DISCUSSION

Conformational Stability of Grx2. E. coli Grx2 is a monomeric, two-domain protein implying that there are three components that could contribute to its stability: the intrinsic stabilities of the two nonidentical domains and the interactions at the domain−domain interface. Previous studies with GSTs have suggested that the smaller domain 1 is less stable than domain 2 (*12, 23*), which could lead to noncooperative unfolding. At equilibrium, unfolding of Grx2 is characterized by a single transition with overlaying fluorescence and CD data having an m value that is 1.6−2.5 times larger than that predicted for the individual domains. The m value correlates well with the amount of surface area that becomes exposed to solvent when the entire Grx2 molecule unfolds. These findings are consistent with an equilibrium two-state process in which the two domains unfold and refold as a single, cooperative unit. The stabilities of the individual domains of Grx2 are, therefore, tightly coupled to domain−domain interactions. The interface between the two domains is extensive and predominantly hydrophobic, involving the burial of a substantial amount of surface area. This could explain the failed attempts to prepare folded domain 1 in a manner independent of domain 2 (*13*). The entropic penalty resulting from the folding of Grx2 would be offset, at least in part, by a gain in enthalpy arising from extensive interdomain contacts.

Contribution of Domains in GSTs. Because the structure of Grx2 closely resembles that of the canonical subunit of dimeric GSTs, intersubunit interactions may not be essential for the association of the two domains in each GST subunit. This is supported by the finding that a monomeric, mutant form of a class mu GST displays a nativelike conformation (*12*). Furthermore, a cooperative link was identified between the domains of the GST by amide hydrogen−deuterium exchange mass spectrometry involving helix 1 in domain 1 and helix 6 (corresponding to helix 8 in Grx2) in domain 2 (*12*). Although stability studies with dimeric GSTs suggest

that domains 1 and 2 could behave cooperatively (*24*−*27*), interdomain contacts are also involved in the assembly and stability of the dimers (*10*). This study is the first with a wild-type monomeric form of a GST-like protein to demonstrate that the two structurally distinct domains behave as a single cooperative folding unit without any influence from quaternary interactions. Intersubunit interactions are, however, important determinants of the stability of the two-domain subunits of dimeric GSTs. The construction of dimeric GSTs from a stable, monomeric precursor could allow for the intrinsic stability of individual subunits to decrease as the stabilizing effects of quaternary interactions become increasingly important. The finding that evolutionarily newer subunits are intrinsically less stable than older subunits suggests that the functionality of the GST dimer is most likely the major evolutionary pressure rather than enhanced subunit stability (*8*). The enhanced conformational flexibility required by GSTs to achieve high levels of functional promiscuity appears to involve greater conformational heterogeneity at the domain interface (*4*).

Unfolding Pathway of Grx2. Whereas Grx2 unfolds in a cooperative two-state manner at equilibrium, kinetics data indicate a more complex unfolding pathway. The unfolding kinetics are characterized by two observable processes, a major fast phase and a minor slow phase. According to the data from this study, we propose the following model for the unfolding of Grx2: major track, N_f (80%) → U_{cis} (50%) ↔ U_{trans} (30%); minor track, N_s (20%) → U (20%), where N_f and N_s represent two native species that unfold, in parallel, on a fast track (f subscript) and slow track (s subscript), respectively. U_{cis} and U_{trans} are unfolded Grx2 with *cis*- and *trans*-Pro49, respectively. The numbers in parentheses represent the relative population of each state. The spectroscopically silent *cis*−*trans* proline isomerization reaction (U_{cis} ↔ U_{trans}) on the fast track is detected in interrupted unfolding experiments. Further, there is no evidence indicating that unfolding proceeds via a high-energy intermediate that might suggest independent unfolding of the domains in Grx2. The kinetics data are, therefore, consistent with the existence of extensive cooperativity between the two domains, in agreement with the equilibrium data. This study provides the first evidence of native-state heterogeneity in the family of GST-like proteins. However, the origin of the heterogeneity in the native state of Grx2 is unclear. The weak denaturant dependence of the minor slow unfolding phase points to a small change in the exposure of surface area and is consistent with the rate of N_s unfolding being limited by an undetermined structural isomerization reaction. Distinct nativelike forms of other proteins that differ mainly in the *cis*−*trans* isomerism about a peptidyl−proline bond and that give rise to kinetic heterogeneity have been observed previously (*28*−*30*). NMR spectroscopy, however, does not indicate any conformational heterogeneity at proline residues in folded Grx2 (*6*).

SUPPORTING INFORMATION AVAILABLE

Unfolding and refolding transitions of Grx2 monitored by fluorescence at 340 nm and CD ellipticity at 222 nm (Figure S1) and recovery of fluorescence and far-UV CD spectra following the refolding of urea-denatured Grx2 (Figure S2). This material is available free of charge via the Internet at http://pubs.acs.org.

REFERENCES

1. Sheehan, D., Meade, G., Foley, V. M., and Dowd, C. A. (2001) Structure, function and evolution of glutathione transferases: Implications for classification of non-mammalian members of an ancient enzyme superfamily. *Biochem. J. 360*, 1–16.
2. Oakley, A. J. (2005) Glutathione transferases: New functions. *Curr. Opin. Struct. Biol. 15*, 716–723.
3. Dirr, H., Reinemer, P., and Huber, R. (1994) X-ray crystal structures of cytosolic glutathione *S*-transferases. Implications for protein architecture, substrate recognition and catalytic function. *Eur. J. Biochem. 220*, 645–661.
4. Hou, L., Honaker, M. T., Shireman, L. M., Balogh, L. M., Roberts, A. G., Ng, K. C., Nath, A., and Atkins, W. M. (2007) Functional promiscuity correlates with conformational heterogeneity in A-class glutathione S-transferase. *J. Biol. Chem. 282*, 23264–23274.
5. Wilce, M. C., and Parker, M. W. (1994) Structure and function of glutathione *S*-transferases. *Biochim. Biophys. Acta 1205*, 1–18.
6. Xia, B., Vlamis-Gardikas, A., Holmgren, A., Wright, P. E., and Dyson, H. J. (2001) Solution structure of *Escherichia coli* glutaredoxin-2 shows similarity to mammalian glutathione-*S*-transferases. *J. Mol. Biol. 310*, 907–918.
7. Ladner, J. E., Parsons, J. F., Rife, C. L., Gilliland, G. L., and Armstrong, R. N. (2004) Parallel evolutionary pathways for glutathione transferases: Structure and mechanism of the mitochondrial class κ enzyme rGSTK1-1. *Biochemistry 43*, 352–361.
8. Dirr, H. (2001) Folding and assembly of glutathione transferases. *Chem.-Biol. Interact. 133*, 19–23.
9. Neet, K. E., and Timm, D. E. (1994) Conformational stability of dimeric proteins: Quantitative studies by equilibrium denaturation. *Protein Sci. 3*, 2167–2174.
10. Luo, J. K., Hornby, J. A., Wallace, L. A., Chen, J., Armstrong, R. N., and Dirr, H. W. (2002) Impact of domain interchange on conformational stability and equilibrium folding of chimeric class μ glutathione transferases. *Protein Sci. 11*, 2208–2217.
11. Han, J. H., Batey, S., Nickson, A. A., Teichmann, S. A., and Clarke, J. (2007) The folding and evolution of multidomain proteins. *Nat. Rev. Mol. Cell Biol. 8*, 319–330.
12. Thompson, L. C., Walters, J., Burke, J., Parsons, J. F., Armstrong, R. N., and Dirr, H. W. (2006) Double-mutation at the subunit interface of glutathione transferase rGSTM1-1 results in a stable, folded monomer. *Biochemistry 45*, 2267–2273.
13. Vlamis-Gardikas, A., Aslund, F., Spyrou, G., Bergman, T., and Holmgren, A. (1997) Cloning, overexpression, and characterization of glutaredoxin 2, an atypical glutaredoxin from *Escherichia coli*. *J. Biol. Chem. 274*, 11236–11243.
14. Pemble, S. E., Wardle, A. F., and Taylor, J. B. (1996) Glutathione *S*-transferase class Kappa: Characterization by the cloning of rat mitochondrial GST and identification of a human homologue. *Biochem. J. 319*, 749–754.
15. Perkins, S. J. (1986) Protein volumes and hydration effects. The calculations of partial specific volumes, neutron scattering match-points and 280-nm absorption coefficients for proteins and glycoproteins from amino acid sequences. *Eur. J. Biochem. 157*, 169–180.
16. Pace, C. N. (1986) Determination and analysis of urea and guanidine hydrochloride denaturation curves. *Methods Enzymol. 131*, 266–280.
17. Myers, J. K., Pace, C. N., and Scholtz, J. M. (1995) Denaturant *m*-values and heat capacity changes: Relation to changes in accessible surface areas of protein unfolding. *Protein Sci. 4*, 2138–2148.
18. Soulages, J. L. (1998) Chemical denaturation: Potential impact of undetected intermediates in the free energy of unfolding and m-values obtained from a two-state assumption. *Biophys. J. 75*, 484–492.
19. Wallace, L. A., and Matthews, C. R. (2002) Sequential vs. parallel protein-folding mechanisms: Experimental tests for complex folding reactions. *Biophys. Chem. 101*−*102*, 113–131.
20. Tanford, C. (1968) Protein denaturation. *Adv. Protein Chem. 23*, 121–282.
21. Hagerman, P. J., and Baldwin, R. L. (1976) A quantitative treatment of the kinetics of the folding transition of ribonuclease A. *Biochemistry 15*, 1462–1473.

22. Brandts, J. F., Halvorson, H. R., and Brennan, M. (1975) Consideration of the possibility that the slow step in protein denaturation reactions is due to cis-trans isomerizations of proline residues. *Biochemistry 14*, 4953–4963.
23. Dragani, B., Iannarelli, V., Allocati, N., Masulli, M., Cicconetti, M., and Aceto, A. (1998) Irreversible thermal denaturation of glutathione transferase P1-1. Evidence for varying structural stability of different domains. *Int. J. Biochem. Cell Biol. 30*, 155–163.
24. Dirr, H. W., and Reinemer, P. (1991) Equilibrium unfolding of class pi glutathione *S*-transferase. *Biochem. Biophys. Res. Commun. 180*, 294–300.
25. Erhardt, J., and Dirr, H. (1995) Native dimer stabilizes the subunit tertiary structure of porcine class pi glutathione S-transferase. *Eur. J. Biochem. 230*, 614–620.
26. Kaplan, W., Husler, P., Klump, H., Erhardt, J., Sluis-Cremer, N., and Dirr, H. (1997) Conformational stability of pGEX-expressed *Schistosoma japonicum* glutathione S-transferase: A detoxification enzyme and fusion-protein affinity tag. *Protein Sci. 6*, 399–406.
27. Wallace, L. A., Sluis-Cremer, N., and Dirr, H. W. (1998) Equilibrium and kinetic unfolding properties of dimeric human glutathione transferase A1-1. *Biochemistry 37*, 5320–5328.
28. Evans, P. A., Dobson, C. M., Kautz, R. A., and Hatfull, G. (1987) Proline isomerization in staphylococcal nuclease characterised by NMR and site-directed mutagenesis. *Nature 329*, 266–268.
29. Sugawara, T., Kuwajima, K., and Sugai, S. (1991) Folding of staphylococcal nuclease A studied by equilibrium and kinetic circular dichroism spectra. *Biochemistry 30*, 2698–2706.
30. Rousseau, F., Schymkowitz, J. W., Sánchez del Pino, J. W., and Itzhaki, L. S. (1998) Stability and folding of the cell regulatory protein p13(suc1). *J. Mol. Biol. 284*, 503–519.
31. DeLano, W. L. (2002) The PyMOL Molecular Graphics System, DeLano Scientific, LLC, San Carlos, CA.

BI801272T